Egyptian Journal of Radiology and Nuclear Medicine

RESEARCH Open Access

The role of combined diffusion weighted imaging and magnetic resonance cholangiopancreatography in the differential diagnosis of obstructive biliary disorders

Shaimaa Rabie[1*], Ahmed Mohallel[1], Samer Saad Bessa[2], Ahmed Hafez[1] and Amr Magdy El-Abd[1]

Abstract

Background: The aim of this retrospective study was to highlight the role of adding DWI to the conventional MRCP in differentiating benign and malignant obstructive biliary pathologies. MRCP is a non-invasive modality for investigating the morphological features of the pancreaticobiliary system. It can provide indirect evidence of a malignant lesion, such as irregularity of the inner border and abrupt stenosis, with shouldering of the edge suggesting cholangiocarcinoma, while a short segment with regular margin and symmetric narrowing suggests a benign cause. Although these findings are highly sensitive, they are not specific. DWI can complement morphological information obtained by conventional MRCP by providing additional functional information concerning the alteration of tissue cellularity due to pathological processes.

Results: The overall accuracy of the diagnosis, sensitivity, and specificity of the conventional MRCP in differentiation between the benign and malignant biliary structures was significantly increased by combing it with the DWI.

Conclusions: Adding DWI to conventional MRCP significantly improved the diagnostic accuracy regarding the characterization of differentiating benign and malignant biliary strictures.

Keywords: MRCP, DWI/ADC, Biliary strictures

Background

A wide spectrum of disorders affects the biliary tract, mainly categorized into two main interties: benign and neoplastic conditions [1].

The biliary obstructive disease presents a diagnostic challenge, especially when no etiology can be ascertained after laboratory evaluation, abdominal imaging, and endoscopic retrograde cholangiopancreatography (ERCP) sampling [2].

Biliary tract imaging is very important in determining the location, etiology, and severity of the disorder and any related complications. Imaging also guides the management of biliary tract disease and any resulting complications [3].

MRCP has become the standard noninvasive technique for the investigation of the biliary tree to visualize ductal dilatation, strictures, and intraluminal filling defects. It is a highly specific tool for the detection of biliary stones in cases of calcular obstructive jaundice [4].

MRCP is a non-invasive modality for investigating the morphological features of the pancreaticobiliary system. When T2-weighted sequences and MRCP images are evaluated together, detailed information can be obtained in the evaluation of extra-ductal causes of biliary obstruction, which provides an important advantage of

* Correspondence: shaima.rabi3@gmail.com
[1]Departmant of Diagnostic and Interventional Radiology, Faculty of Medicine, Alexandria University, Alexandria, Egypt
Full list of author information is available at the end of the article

MRCP over ERCP. In addition, there is no need for contrast and sedation with MRCP, as opposed to ERCP [5].

MRCP can provide indirect evidence of a malignant lesion, such as irregularity of the inner border and abrupt stenosis, with shouldering of the edge suggesting cholangiocarcinoma, while a short segment with regular margin and symmetric narrowing suggests a benign cause. Although these findings are highly sensitive, they are not specific [6, 7]. Also, signal characteristics of a stenosing biliary lesion on T2-weighted MR (T2WI) images may differentiate between benign and malignant pathology. In general, malignancy appears as a hyper-intense mass-like lesion and the signal intensity of the lesions should be cautiously assessed in most cases, due to the very small tumor size of these infiltrating lesions, and not all tumors will produce a notably high T2 signal [8].

DWI can complement morphological information obtained by conventional MRCP by providing additional functional information concerning the alteration of tissue cellularity due to pathological processes [9].

DWI is based on the random motion of water molecules in tissue. The degree of restriction to water molecule diffusion is directly associated with tissue cellularity and cell membrane integrity. Tumors with increased cellularity show more restricted movement of water molecules than in less cellular tumors [9].

The degree of restricted diffusion is proportional to the degree of signal intensity in DWI. DWI should always be confirmed with an ADC map. The ADC map is a quantitative parameter calculated from DWI. Higher signal intensities in DWI and lower ADC values are defined as the result of restricted diffusion. On the other hand, higher ADC values indicate less cellularity of lesions [10].

When DWI is added to the routine biliary MRI protocol, it can provide additional clinically important information for the characterization of biliary strictures or peri-ampullary tumors; differentiation of malignant from benign tumor-like lesions in the biliary tract also can improve the detection of abnormal lesions and the evaluation of the tumor extent along the bile tree [11].

Methods

This prospective study included 60 patients who were referred to the department of radiodiagnosis for MRI evaluation of the biliary tree complaining of obstructive jaundice with no definite diagnosis made by the prior investigation.

All patients were subjected to full history taking and review of their previous laboratory investigations as liver function tests (LFTs), or radiologic investigations as ERCP and hepato-biliary ultrasound (US) examination.

Patient preparation

Fasting was requested for at least 6 h before the examination to promote gall bladder filling and gastric emptying and to reduce unwanted fluid signals from the intestine. Sedation with oral chloral hydrate was given to children aged younger than 6 years or those who were not able to cooperate during the examination. Patients were instructed to control their breath according to the technician's instructions.

Exclusion criteria were (a) Patient with a known history of primary biliary neoplasm, (b) rapid or irregular respiratory pattern due to liver failure with tense ascites, (c) degraded images by excessive motion artifacts on DWI, and (d) absolute contraindications for MRI (e.g., permanent metallic processes and pacemakers).

MR imaging protocol

All the MRI examinations were done between January 2017 and February 2020. The MRI examinations of the upper abdomen were performed by a Siemens Sempra 1.5 T closed magnet, using a phased-array body surface coil.

The conventional pancreaticobiliary MRI protocol consisted of the following sequences: T2-weighted fast spin-echo sequence on axial and coronal planes; three-dimensional, fat-suppressed, heavily T2-weighted fast spin-echo sequence with multi-slab acquisition mode; two-dimensional thick single slab projectional images; three-dimensional reconstruction algorithms; and unenhanced and contrast-enhanced dynamic spoiled 3D GE sequences were done for few cases when requested by their referring physician. The detailed imaging parameters are summarized in Table 1.

In the current exam, respiratory or navigator triggered/controlled techniques synchronize data acquisition with respiratory movement, and data are acquired only within a certain period of the respiratory cycle (usually the expiratory phase). The advantages of this method include better subjective image quality, higher SNR, higher lesion-to-parenchymal contrast ratio, and more precise ADC quantification compared with breath-hold DWI. The detailed imaging parameters are summarized in Table 2.

The apparent-diffusion coefficient (ADC) map was calculated using a monoexponential function with b values of 0, 400, and 800 s/mm^2. However, in some cases, the ADC values were difficult to be evaluated due to the extremely small size of the lesion precluded the reliable measurement of the region of interest.

Image analysis

Results of MRCP were reviewed separately by two experienced radiologists in gastrointestinal blinded to the

Table 1 Imaging parameters for MRCP sequences

	T2WI FSE with fat saturation	Coronal thick-slab single slice TSE sequence	3D RT-T2W TSE sequence
Repetition time (m/s)	200	1800	2500
Echo time (m/s)	80	677	680
Echo train length	23	256	69
Flip angle	90	130	90
Matrix	320	256 × 160	384
Field of view (mm^2)	400	380 × 380	400
Section thickness (mm)	6	4	1
Respiratory compensation	Respiratory gated		
Acquisition time	**2 min**	**1 min 20 s**	3 min 30s

final diagnosis but having only clinical information related to the symptoms of patients.

Two sets of images are reviewed separately: (1) MRCP and T2WI and (2) MRCP, T2, and DWI.

A comment on the following variables was done on each case: (1) diameter of the CBD, (2) length of the stricture, (3) shape and borders of the stricture, (4) presence of double duct sign, (5) visible soft tissue lesion causing the obstruction, (6) the signal intensity (SI) on T2 signal, and (7) SI on DWI and ADC maps.

The criteria predictive for malignancy were a long segment of stenosis, asymmetrical irregular margins of the stricture, abrupt transitions of the bile duct caliber, SI higher than the liver on T2 images, and high SI on DWI (with high b values) with corresponding low SI on ADC maps.

ADC values were estimated; however, in some cases, the ADC values were difficult to be evaluated because the very small size of the lesion precluded the reliable measurement of the region of interest.

Table 2 Imaging parameters for DWI

Parameters	SE-EPI-DWI (1.5 T MRI)
Sequence	Single-shot spin-echo echo-planner
Imaging plane	Axial
TR/TE	1500/80
FA	90
FOV	380
Slice thickness	6
Intersection gap	0
Reconstruction matrix	252
Band width	2233.8
NSA	2
Parallel imaging (SENSE)	Yes
***B* values**	3 (0, 400, and 800)
Acquisition time	2:30 (min:s)

Confirmation of the diagnosis

A blind review was done first, and then the provisional MRCP diagnosis was compared with the final diagnosis based on patient's management either by further investigation, pathological correlation, or surgical and ERCP data.

Results

The current study included 60 patients, distributed equally as 30 females and 30 males, their ages ranged between 12 years and 80 years with a mean age was 49.5±16.3 years. Among the 60 patients, there were 34 patients with a final diagnosis of benign pathology and 26 patients with malignant lesions.

The benign conditions included; congenital, inflammatory, postoperative complications, extrinsic biliary compression by benign lesions, sphincter of Oddi dysfunction, and ampullary stenosis. Regarding the malignant conditions, they included pancreatic adenocarcinoma, hepatic and extrahepatic cholangiocarcinoma, gall bladder cancer, peri-ampullary carcinoma, pathological lymph nodes infiltrating the CBD, infiltrative HCC, and hepatic deposits showing biliary invasion; all the cases were distributed as in Table 3.

Regarding the patients with congenital disorders including choledocal cysts and Todani type IA and type IC; one is confirmed by a follow-up MRCP study done after 3 months, showing stationary conditions, and the other one had milder dilatation and followed up by the US, which also showed stationary condition.

Among the patients with inflammatory pathologies, there were 4 cases diagnosed as IGg4-related biliopancreatitis, 5 cases with sclerosing cholangitis, one case with ascending cholangitis secondary to distal begin CBD stricture, and one case with acute interstitial edematous pancreatitis; they were confirmed by clinical and laboratory data and six of cases had follow-up MRCP study within 3 months to a 1-year interval (Figs. 1 and 2).

Table 3 Distribution of the cases according to their pathology

Benign pathological entity	No. of cases (*n*)	Malignant pathological entity	No. of cases (*n*)
Congenital	2	Pancreatic cancer	10
Inflammatory	12	Intrahepatic cholangiocarcinoma	6
Post-operative complication	5	Peri-ampullary cancer	3
Sphincter of Oddi dysfunction/ampullary stenosis	10	Pathological porta hepatis nodes	2
Benign extrinsic biliary compression	5		
Total	**34**	HCC	1
		GB cancer	1
		Hepatic deposits from gastric cancer with biliary invasion	1
		Extrahepatic CBD cholangiocarcinoma	2
		Total	**26**

The other cases with inflammatory pathology were xanthogranulomatous cholecystitis with multiple gall bladder and CBD stones.

Two out of four cases with postoperative complications were hilar anastomotic strictures following hepatic transplantation: one in liver recipient patient and the other one was in hepatic donor patient; both were confirmed by ERCP. One case was post-choledocojujenostomy as management of complicated cholecystectomy in a patient with managed breast cancer and was followed by contrast-enhanced triphasic CT showing no detected suspicious enhancing lesions.

The two other cases of the postoperative complication were post-cholecystectomy stricture and were classified as Bithmus II and Bithmus III strictures. Ten of the benign cases were diagnosed as sphincter of Oddi dysfunction and ampullary stenosis and were confirmed either by ERCP and or by follow-up with symptom resolution after conservative medical treatment.

Five cases of benign biliary obstruction were caused by eccentric compression; two were Mirrizi syndrome, one case was caused by an obstructing 2nd part duodenal diverticulum (confirmed by CT) (Fig. 3). One case was pancreatic head serous-cystadenoma, and the last case was portal biliopathy with compression of the CBD by the dilated tortuous portal vein.

Among the malignant cases, 15 patients were confirmed by histopathology (Figs. 4 and 5), 2 cases confirmed by contrast-enhanced dynamic MRI revealing positive enhancing lesions, 4 cases underwent contrast-enhanced triphasic CT studies, 2 cases confirmed by ERCP with no available histopathological data, and 4 patients had advanced malignancy with metastasis underwent palliative stenting and died before histopathological confirmation.

All the patients had biliary dilatation; among them, 15 cases had intrahepatic dilatation only and 45 cases had intra- and extrahepatic dilatation. The degree of biliary dilation in the cases with mixed intra- and extrahepatic biliary dilatation estimated by measuring the CBD caliber, and was significantly larger in the malignant cases; ranged among the benign cases between 6 mm and 18 mm with a mean caliber of 12.67 ± 3.34, and among the malignant cases ranged between 12 and 22 mm with a mean caliber of 17.0 ± 3.31 mm.

In cases with intrahepatic biliary dilatation, the degree of biliary dilatation showed no significant difference between the benign and malignant pathologies; the caliber of the dilated intrahepatic biliary ducts ranged between 4 and 15 mm (mean ± SD.8.0 ± 3.56 mm) among the benign cases and 6 mm and 13 mm (mean ± SD.9.50 ± 2.39 mm) among the malignant cases (Table 4).

The stricture length was significantly longer among the malignant cases compared to the benign cases, ranging between 3 and 26 mm (mean ± SD 8.34 ± 5.62 mm). The malignant cases ranged between 7 to 40 mm (mean ± SD 22.04 ± 8.08 mm) (Table 3).

The presence of the double duct sign in cases with distal biliary extrahepatic obstruction was significantly higher among the malignant cases; it was present in 14 out of 18 malignant cases and in 6 out of 27 benign cases. Among the benign cases, it was detected in 4 cases with IGg4-related cholangitis, one case with ampullary stenosis, and one case with distal biliary compression with duodenal diverticulum.

The shape of the strictures was described in the conventional MRCP regarding the following criteria: luminal regularity, border symmetry, and the shape of the transition to the aberrantly normal more distal biliary tree, the finding of luminal irregularity, asymmetry of the borders, and the abrupt narrowing were significantly higher in the malignant cases (Table 5).

Regarding the signal intensity (SI) of the strictures on T2 weighted images, they were categorized as iso, hypo, and hyperintense in relation to the hepatic parenchyma, and the finding of T2 hyper-intensity was significantly higher among the malignant lesions compared to the benign lesions (Table 6).

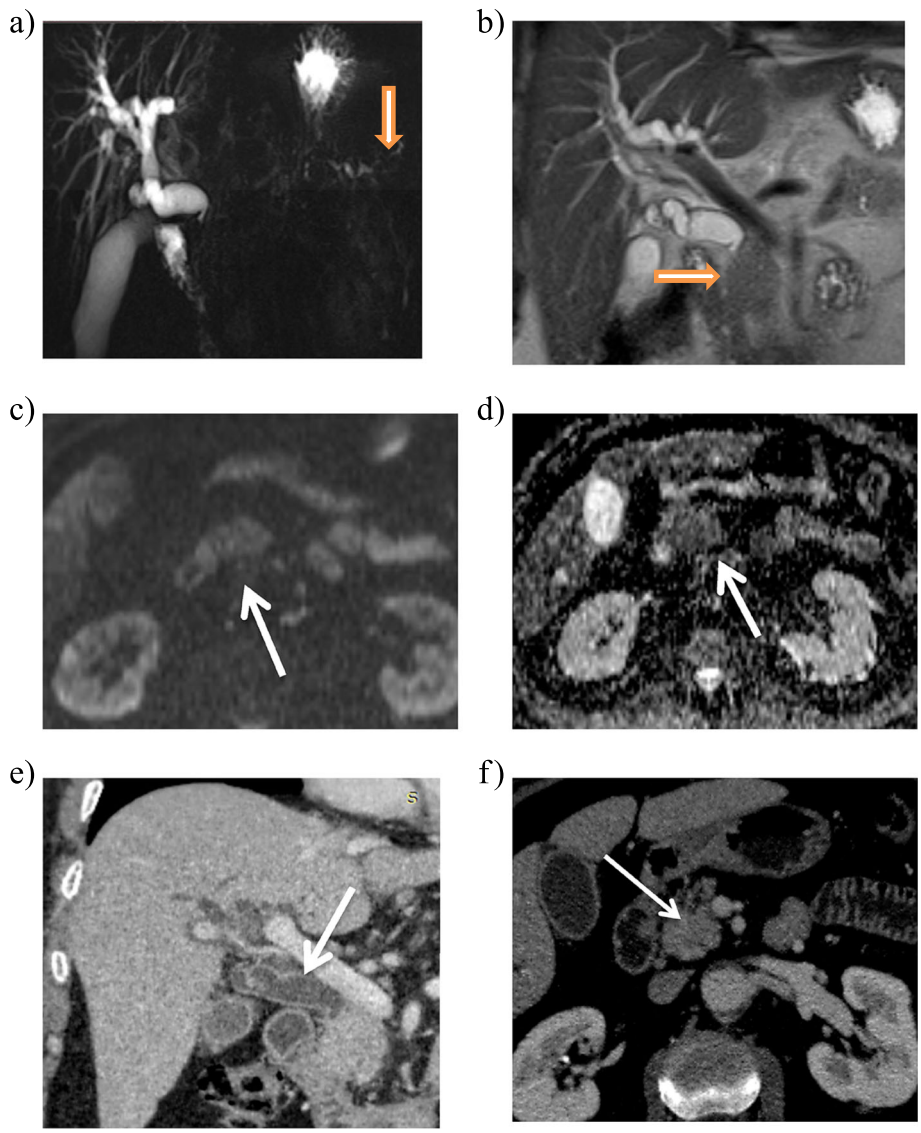

Fig. 1 A 65-year-old male patient with IGg4 related bilio-pancratitis. **a** 3D T2 coronal thick slab MRCP image showing intra- and extrahepatic biliary dilation with distal CBD (intra-pancreatic segment) long strictures (25 mm), showing regular borders still abrupt transition, multifocal strictures, and ectasia of the main and side pancreatic ducts (thick arrow). **b** Coronal T2 HASTE showing an ill-defined iso-intense 2 cm lesion at the pancreatic head at the site of the stricture (thick arrow). **c**, **d** DWI and ADC map showing no restricted diffusion (thin arrows). **e** Coronal contrast enhanced CT image showing abnormal smooth enhancement of the distal CBD (long arrow). **f** Axial contrast enhanced CT image showing ill-defined hypo-enhancing pancreatic head lesion (thin arrow)

Regarding the SI on high *b* value DWI (*b* 800) and ADC maps, hyperintensity on DWI with a corresponding hypointensity on ADC maps is considered as a positive diffusion restriction and was significantly higher among the malignant lesions compared to the benign lesions (Table 7).

The ADC values were measured in 22 cases of the malignant lesions and ranged between 0.68×10^{-3} and 1.27×10^{-3} (mean± SD 0.87×10^{-3}). In the remaining two cases the lesions were very small precluded accurate measurement of the ADC values. In the benign lesions the ADC value was measured in 24 of the cases, and ranged between 1.4×10^{-3} and 2.9×10^{-3} (mean± SD 2.13×10^{-3}). In the remaining cases the lesions were very small (less than 5 mm) precluded the accurate measurement of the ADC values. By using Roc curve analysis, the ADC cutoff value to differentiate between the benign and malignant lesions which has the highest sensitivity (100%) and specificity (100%) was ≤ 1.27.

Conventional MRCP correctly diagnosed 30 cases of benign cases and misdiagnosed two cases as malignant strictures, and another case was equivocal. MRCP also

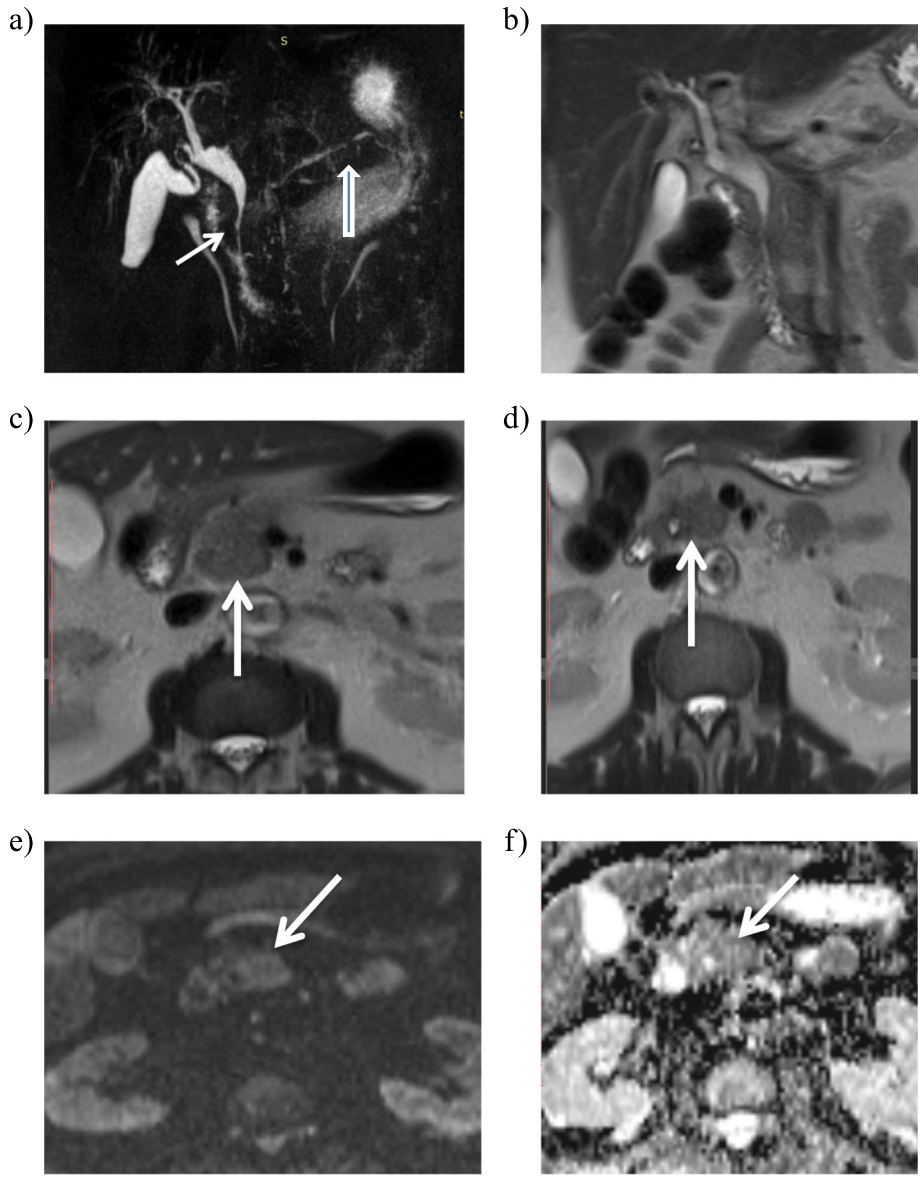

Fig. 2 Follow-up study for the same patient three months later. **a**, **b** 3D T2 coronal thick slab MRCP and coronal HASTE images showing partial regression of the degree of biliary dilatation (CBD=12 m), as well as the main pancreatic duct (thick arrow) and the biliary stricture (thin arrow). **c** Initial and follow up axial T2 HASTE images showing resolution of the pancreatic head mass (white arrows). **d** DWI and ADC map, still showing no diffusion restriction (thin arrows)

correctly diagnosed 23 out of 26 malignant cases; three cases were misdiagnosed as benign strictures. Thus, the overall rate of correct diagnosis (accuracy rate) was 88.33% (53/60) (Table 6).

While DWI/ADC correctly diagnosed all the 34 benign cases, also DWI correctly diagnosed 24 of the malignant cases and misdiagnosed 2 cases because of the small size of the lesion in these two cases. Thus the overall rate of correct diagnosis (accuracy rate) was 96.67% (58/60) (Table 8).

The first case was a mid-CBD stricture showing malignant MRCP features with no detected DWI restriction, contrast-enhanced CT study revealed mural thickening and enhancement at the site of the stricture, and it was confirmed by ERCP and histopathology to be malignant stricture (cholangiocarcinoma). The second case was intrahepatic hilar peri-ductal infiltrative cholangiocarcinoma, showing malignant MRCP features with no definite diffusion restriction on DWI, confirmed by ERCP to be malignant stricture.

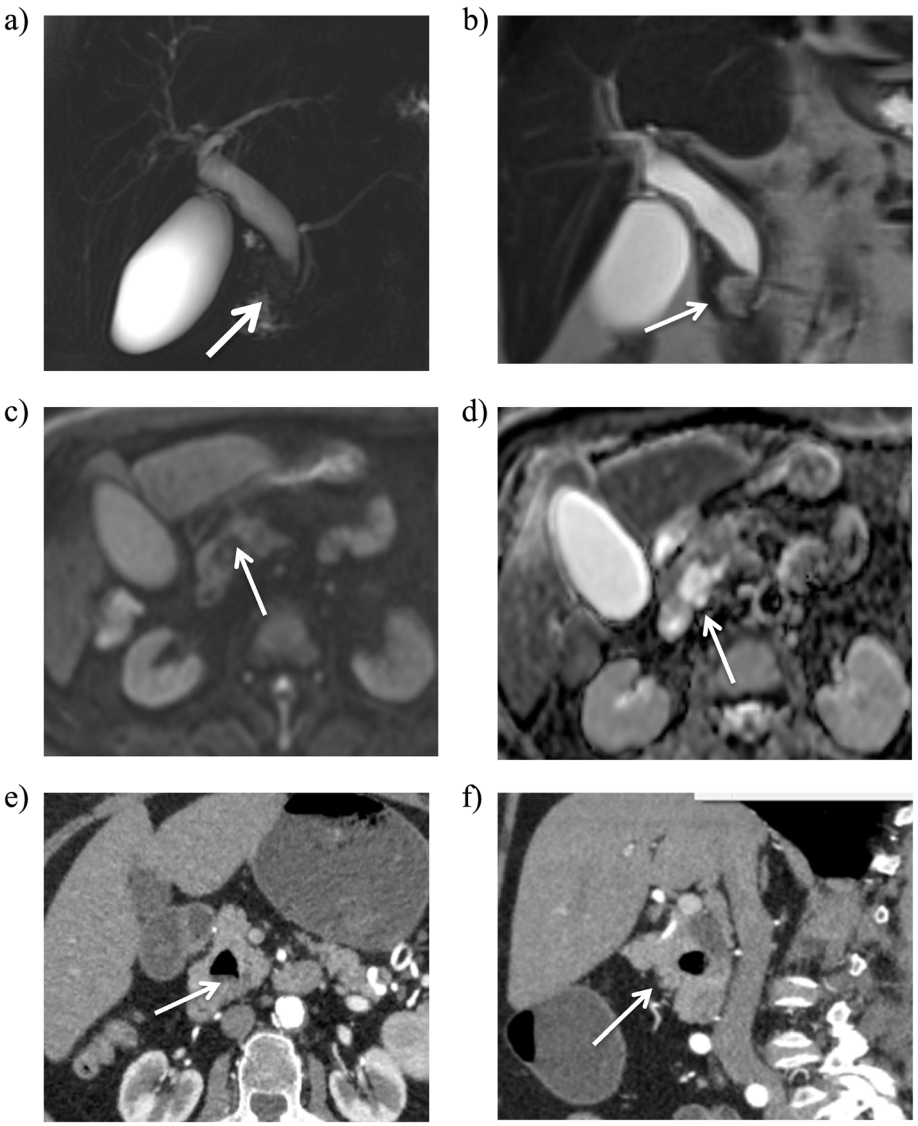

Fig. 3 A 40-year-old female patient complaining of obstructing jaundice. **a** 3D T2 coronal thick slab MRCP image showing intra- and extrahepatic biliary dilatation with distal CBD stricture at the peri-ampullary region showing rather regular relatively asymmetrical borders (arrow), also with mild dilatation of the MPD. **b** Coronal T2 HASTE images showing a hyper-intense mass like lesion at the site of the stricture averaging 2 cm (arrow). **c**, **d** DWI and ADC maps showing no restricted diffusion (arrows). **e**, **f** Axial and sagittal contrast enhanced CT images revealing a small 2nd part duodenal diverticulum causing the biliary dilatation (arrows)

DWI also increased the detection and diagnosis of hepatic deposits, the pathological retroperitoneal and porta-hepatis nodes that were undetected or equivocal on the conventional MRCP and T2 sequences in 5 of the malignant cases.

The combination of both MRCP and DWI correctly diagnosed 34 of the benign cases and 25 of the malignant lesions with the overall accuracy rate was 98.33% (59/60) (Table 6). The diagnostic sensitivity and specificity of MRCP were 88.46% and 88.24%, respectively. Whereas, for DWI, the diagnostic sensitivity and specificity were 92.31% and 100%, respectively (Table 7). So the addition of DWI to the conventional MRCP protocol changes the final diagnosis in 5 out of 60 cases (8.3%) and increased their sensitivity and specificity (Table 9).

Discussion

It is of great importance to accurately detect bile duct and pancreatic duct abnormalities in patients with obstructive jaundice as it helps both surgeons and endoscopists to take care of such patients and plan further line of management [12].

MRCP has become the standard noninvasive technique for the investigation of the biliary tree to visualize

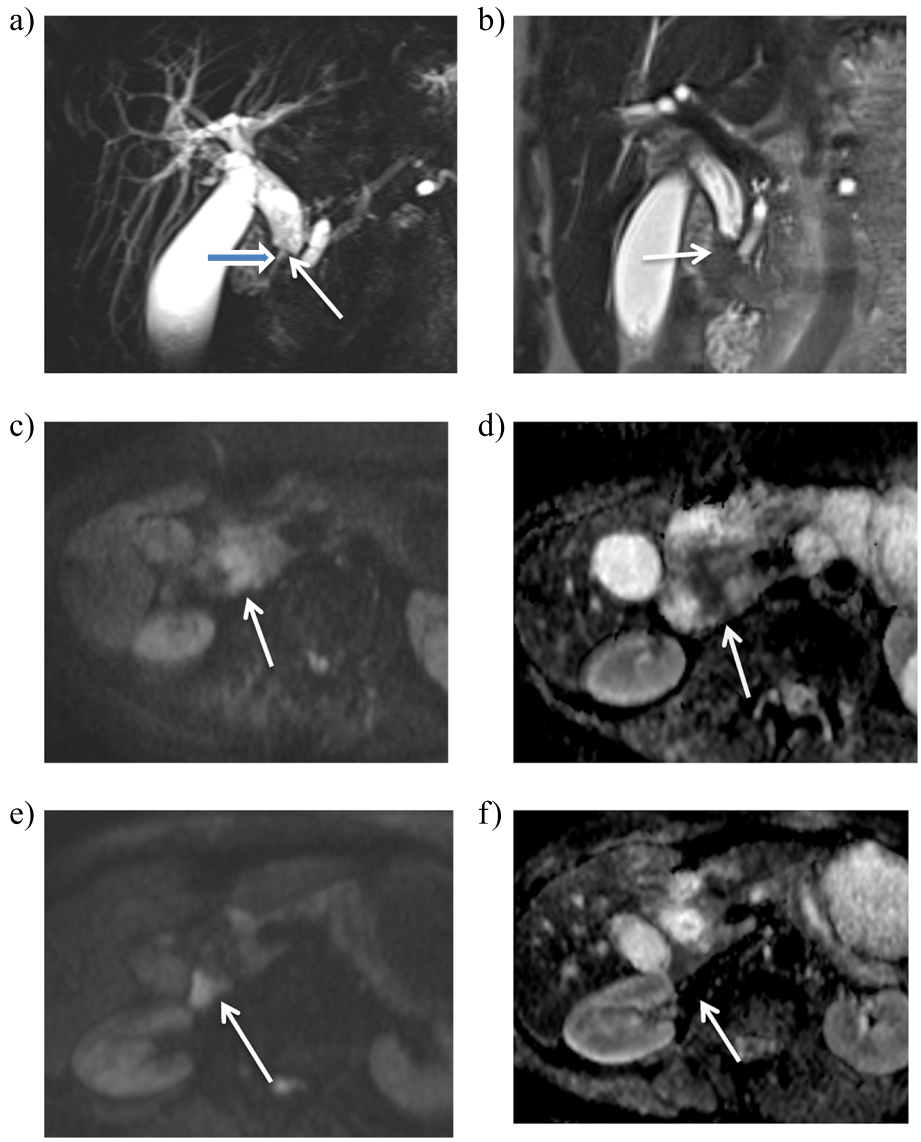

Fig. 4 A 65-year-old patient diagnosed with pancreatic head adenocarcinomas. **a** 3D T2 coronal thick slab MRCP image showing double duct sign and distal intra pancreatic segments CBD stricture showing irregular asymmetrical border with abrupt narrowing (thick arrow), biliary stent is noted crossing the stricture (thin arrow). **b** Coronal T2 HASTE image at the level of the stricture showing iso-intense signal (arrow). **c**, **d** DWI and ADC map at the same level showing hyperintense signal on DWI with corresponding hypo-intensity on the ADC map (restricted diffusion) (arrows). **e**, **f** DWI and ADP map at lower level showing restricted retroperitoneal lymph node that was undetected on the T2 images (arrows)

ductal dilatation, strictures, and intraluminal filling defects. It provides noninvasive images comparable to those obtained by direct retrograde or trans-hepatic cholangiography [8].

However, MRCP is a safer technique without the risks for complications associated with the ERCP such as pancreatitis, cholangitis, hemorrhage, and duodenal perforation, as well as the study, involves radiation, contrast material is necessary and there is a requirement for sedation [13].

MRCP can provide indirect evidence of malignant lesions, such as irregularity of the inner border, abrupt stenosis, and stenosis length of the biliary tree. Although these findings are highly sensitive, they are not specific to malignancy [13, 14].

In the current study, we evaluated the value of adding DWI to conventional MRCP in differentiating benign from malignant biliary obstructive pathologies, as DWI has begun to gain wide acceptance from many radiologists as a functional MRI technique that is a useful complementary imaging technique. It has the advantage of requiring a short acquisition-time, without the need for contrast administration.

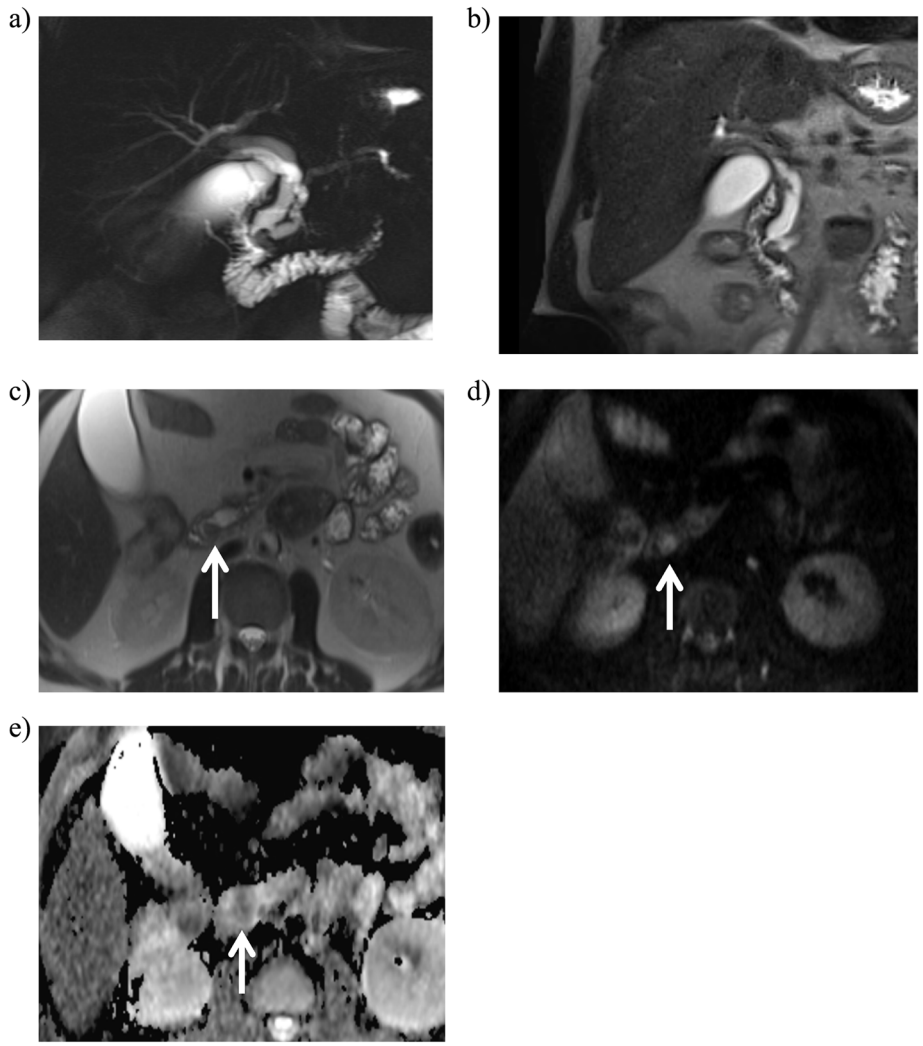

Fig. 5 **a** 3D T2 coronal thick slab images showing intra- and extrahepatic biliary dilatation, double duct sign, and distal CBD stricture showing asymmetrical eccentric narrowing of the CBD and abrupt narrowing of the MPD at the same level. **b**, **c** Coronal and axial T2 HAST sequences showing small iso-intense peri-ampullary lesion (arrow in **c**). **d**, **e** DWI and ADC map showed restricted diffusion at the same level (short arrows). The patient underwent Whipple operation and pathologically proved to be small ampullary adenocarcinoma

Table 4 Comparison between the two studied groups according to the biliary dilatation

Biliary dilatation	Total (*n*=60)		Benign (*n*=34)		Malignant (*n*=26)		Test of sig.	*P*
	No.	%	No.	%	No.	%		
Intrahepatic biliary dilatation	**15**	**25.0**	**7**	**20.6**	**8**	**30.8**		
Intrahepatic duct diameter (mm)								
Min.–Max.	4.0–15.0		4.0–15.0		6.0–13.0		*U*=16.0	0.189
Mean ± SD.	8.80 ± 2.98		8.0 ± 3.56		9.50 ± 2.39			
Median (IQR)	8.0 (7.0–10.50)		7.0 (6.50–8.50)		9.0(8.0–11.50)			
Intra + extra	**45**	**75.0**	**27**	**79.4**	**18**	**69.2**		
CBD diameter (mm)								
Min.–Max.	6.0–22.0		6.0–18.0		12.0–22.0		*t*=4.280*	< 0.001*
Mean ± SD.	14.40 ± 3.93		12.67 ± 3.34		17.0 ± 3.31			
Median (IQR)	14.0 (12.0–16.0)		13.0(9.50–16.0)		17.0(14.0–20.0)			

Table 5 Comparison between the two studied groups according to MRCP features of the stricture

MRCP features of the stricture	Total (*n*=60)		Benign (*n*=34)		Malignant (*n*=26)		Test of sig.	*P*
	No.	%	No.	%	No.	%		
Length (mm)								
Min.–Max.	3.0–40.0		3.0–26.0		7.0–40.0		*U* = 70.0*	< 0.001*
Mean ± SD.	14.28 ± 9.60		8.34 ± 5.62		22.04 ± 8.08			
Median (IQR)	12.0 (6.0–23.0)		6.0 (5.0–10.0)		23.0 (15.0–26.0)			
Borders								
Symmetrical	30	50.0	30	88.2	0	0.0	χ^2=45.882*	< 0.001*
Asymmetrical	30	50.0	4	11.8	26	100.0		
Lumen								
Regular	37	61.7	33	97.1	4	15.4	χ^2=41.576*	< 0.001*
Irregular	23	38.3	1	2.9	22	84.6		
Transition								
Gradual tapering	30	50.0	27	79.4	3	11.5	χ^2=27.149*	< 0.001*
Abrupt narrowing	30	50.0	7	20.6	23	88.5		

χ^2 chi-square test, *U* Mann-Whitney test, *p p* value for comparing between the two studied groups
*Statistically significant at $p \leq 0.05$

Regarding the SI on high *b* value DWI (*b* 800) and ADC maps; a hyperintensity on DWI with a corresponding hypointensity on ADC maps was considered as positive diffusion restriction and was significantly higher among the malignant lesions compared to the benign lesions, 24 of the malignant cases showed restricted diffusion, and only two cases were missed by DWI, these two cases were peri-ductal infiltrative cholangiocarcimona, one was intrahepatic and the other one was extrahepatic mid-CBD cholangiocarcinoma, we believe that they were missed by DWI due to their small size; both were less than 4 mm, on the other hand, none of our benign cases showed diffusion restriction.

A previous study by Tsai et al. [8] included 42 patients with malignant obstructive biliary lesions also reported two false-negative malignant lesions missed by DWI, they were both peri-ductal cholangiocarcinomas located in the left hepatic lobe. Their respective sizes were 1.7 cm and 1.4 cm. They explained this misreading by the lesser diffusion restriction and motion artifact in the left hepatic lobe from the heartbeat. Also, they reported one false-positive malignant peri-ampullary lesion showing a high signal in DWI secondary to the T2 shine-through effect and low spatial resolution of DWI due to intestinal motion artifacts at the 2nd part of the duodenum [8].

Our results were lower than that of Cetiner et al. [12] who reported that all the malignant cases were diagnosed by DWI, all their malignant lesion were correctly diagnosed by DWI with sensitivity and specificity of 100%. This may be due to the larger size of the malignant tumors as their study did not include infiltrative cholangiocarcinoma [12].

In our study ADC values were measured in the malignant strictures except for two cases because the very small size of the lesions precluded accurate measurement of the ADC values, the mean ADC value was 0.87×10^{-3} (range $0.68–1.27 \times 10^{-3}$).

In agreement with our results, Sim et al. investigated the diagnostic efficacy of the DWI in differentiating benign and malignant lesions and reported ADC values of $0.928x\ 10^{-3}$ ($0.841–0.976x10^{-3}$) among the malignant strictures [15].

Cetiner et al. measured the ADC values in fourteen patients with malignant lesions; among them the mean ADC value was $1.306±0.30×10^{-3}$ mm^2/s (range $0.9–1.9×10^{-3}$ mm^2/s), explaining higher values ADC values

Table 6 Comparison between the two studied groups according to T2 signal of the obstructing lesions

T2 signal	Total (*n*=60)		Benign (*n*=34)		Malignant (*n*=26)		χ^2	^{MC}p
	No.	%	No.	%	No.	%		
Hyper	23	38.3	2	5.9	21	80.8	37.333*	< 0.001*
ISO	36	60.0	31	91.2	5	19.2		
Hypo	1	1.7	1	2.9	0	0.0		

χ^2 chi-square test, *MC* Monte Carlo, *p p* value for comparing between the two studied group

Table 7 Comparison between the two studied groups according to the diffusion restriction on DWI and ADC map

	Total (*n*=60)		Benign (*n*=34)		Malignant (*n*=26)		Test of sig.	*P*
	No.	%	No.	%	No.	%		
Restriction on DWI								
−ve	36	60.0	34	100.0	2	7.7	$\chi^2 = 52.308^*$	$< 0.001^*$
+ve	**24**	**40.0**	**0**	**0.0**	**24**	**92.3**		

χ^2 chi-square test, *p* *p* value for comparing between the two studied groups
*Statistically significant at $p \leq 0.05$

seen in low-grade adenocarcinoma and three of their malignant tumors had a cystic component [12].

By using Roc curve analysis the ADC cutoff value to differentiate between the benign and malignant lesions which has the highest sensitivity (100%) and specificity (100%) was ≤ 1.27×10^{-3}.

The previous study by Zhong et al. comparing the accuracy of the different biliary imaging modalities in diagnosing the cause of the biliary obstruction in 82 patients, the accuracy of them was as follows: US (57.3%), CT (73.7%), ERCP (85.0%), and MRCP (87.8%) [16].

Matching with their results in the current study, the MRCP showed 88.3% accuracy in the diagnosis of the biliary obstruction, with 88.4% sensitivity and 88.2% specificity.

Another earlier prospective study by Rosch et al. [17] comparing the diagnostic accuracy of four imaging methods (i.e., ERCP, EUS, MRCP, and CT) reported no statistically significant difference between the sensitively of the MRCP and ERCP for diagnosing malignant strictures, the sensitivity and specificity for the diagnosis of malignancy in the 50 patients were as follows: ERCP showed 85% sensitivity and 75% specificity, the MRCP showed 85% sensitivity and 71% specificity, the CT showed 77% sensitivity and 63% specificity, and finally, the EUS showed 79% sensitivity and 62% specificity.

A few previous studies demonstrated that; the specificity of MRCP for characterizing malignant biliary strictures was improved by combining MRCP with either EUS or contrast-enhanced MRI. Specifically, the combination of MRCP and EUS helped to demonstrate the presence of a visible mass, whereas that of MRCP and contrast-enhanced MRI allowed better depiction of the bile duct walls and extension of malignant lesions [14].

Although combining MRCP and contrast-enhanced MRI or EUS may facilitate the differential diagnosis of biliary strictures, the benefit of using contrast may not outweigh its risk for the development of nephrogenic systemic fibrosis in patients with poor renal function, and the routine use of EUS may also increase the medical costs and complexity of the diagnostic workup [18].

Our results showed that the addition of DWI significantly improved the overall diagnostic accuracy of the conventional MRCP from 88.33 to 98.3% ($P< 0.001$). The addition of DWI led to correct changes of the final diagnosis of 8.3% of the patients (5/60).

The sensitivity and specificity of diagnosis benign and malignant strictures were significantly higher with combined T2WI, MRCP, and DWI than with conventional T2WI and MRCP, with values increasing from 88.4% and 88.2% to 96% and 100%, respectively.

Our results were comparable to the results of a study by Tsai et al. [8] which reported an improvement of the diagnostic accuracy of MRCP by adding the DWI from 93 to 98%, also the diagnostic sensitivity increased from 79 to 98%.

Our study had some limitations. First, in this study, we did not include a dynamic MRI study as a routine part of the examination; it was only done in two of the malignant cases as requested by the referring physician, and their results confirmed our diagnosis revealing enhancing lesions; however, it did not change our final diagnosis.

Therefore, the diagnostic value of a combined MRCP and dynamic study with or without DWI was not investigated; however, in an earlier study by Yoo et al., their results revealed that both the sensitivity and specificity of combined MRCP and DWI did not significantly differ from that of MRCP, DWI, and contrast-enhanced T1WI combined [18].

The second limitation, not all the malignant lesions were confirmed by pathology or ERCP. Four out of our malignant cases had advanced malignancy showing hepatic deposits and non-regional nodal metastasis, and they underwent palliative biliary drainage and died before confirmation; however, they were considered malignant depending on the complementary clinical and laboratory data.

Also, most of our cases with benign strictures were not pathologically confirmed. However, we can confidently assume these cases to be benign because they were stable or regressed on a follow-up study, and some patients had symptoms resolution after conservative medical therapy.

Third, our DWIs were obtained using respiratory-triggered methods with b values of 0, 400, and 800 s/

Table 8 Number of patients with malignant and benign biliary strictures diagnosed by DWI and MRCP

	Conventional MRCP	DWI	Combined MRCP +DWI	Total number of cases (*n*)
Number of correctly diagnosed Benign cases	30 (88.2%)	34 (100%)	34 (100%)	**34**
Number of correctly diagnosed malignant cases	23 (88.5%)	24 (92.3%)	25 (96.2%)	**26**

Table 9 Agreement (sensitivity, specificity, and accuracy) for the three imaging sets

	Benign (n = 34)		Malignant (n = 26)		Sensitivity	Specificity	PPV	NPV	Accuracy
	No.	%	No.	%					
MRCP									
Benign	30	88.2	3	11.5	88.46	88.24	85.19	90.91	88.33
Malignant	4	11.8	23	88.5					
χ^2 (p)	**35.017*** (**< 0.001***)								
DWI									
Benign	34	100.0	2	7.7	92.31	100.0	100.0	94.44	96.67
Malignant	0	0.0	24	92.3					
χ^2 (p)	**52.308*** (**< 0.001***)								
Combined MRCP and DWI									
Benign	34	100.0	1	3.8	96.15	100.0	100.0	97.14	98.33
Malignant	0	0.0	25	96.2					
χ^2 (p)	**56.044*** (**< 0.001***)								

* Statistically significant at $p \leq 0.05$

mm^2. Some authors have demonstrated a preference for respiratory-triggered DWI over breath-hold DWI for focal hepatic lesion detection. However, the relevance of this application is not completely clear with regard to the biliary system and has some disadvantages include poor signal-to-noise ratio (SNR), artifacts due to pulsatility and susceptibility, and only a limited number of b values can be obtained per breath-hold [9].

A study by Lee et al. [19] applied free-breathing EPI DWIs; as non-breath hold DWI techniques provide improved SNR and contrast-to-noise ratios, allowing for higher spatial resolution, thin slice partitions (4–5 mm) are possible so the possibility of multiplanar reformatting, multiple b values can also be easily obtained, but this technique is prone to partial volume averaging artifact and can be time-consuming.

Finally, retrospective studies might exhibit a certain degree of selection bias or recall bias, despite implementing thorough inclusion and exclusion criteria and research methods.

Conclusions

In conclusion, adding DWI to conventional MRCP improved the detection and the characterization of the biliary obstructing diseases and significantly increased the diagnostic accuracy regarding the differentiation between benign and malignant biliary strictures.

The current study results can be of value in routine clinical practice considering that DWI can facilitate the characterization of biliary strictures without greatly compromising the overall image acquisition time or kidney function of patients. Improved accuracy in the characterization of biliary strictures would be of particular importance for patients with benign strictures to avoid unnecessary surgery.

Abbreviations

MRCP: Magnetic resonance cholangiopancreatography; DWI: Diffusion-weighted imaging; ADC: Apparent diffusion coefficient; ERCP: Endoscopic retrograde cholangiopancreatography; CT: Computed tomography; CBD: Common bile duct; US: Ultrasound; SI: Signal intensity

Authors' contributions

SR designed the study; acquired, analyzed, and interpreted the data, performed statistical analysis; and drafted the manuscript. AM and AH revised and edited the manuscript. AM and SS reviewed the manuscript. All authors read and approved the manuscript.

Funding

No sources of funding.

Availability of data and materials

The datasets used and/or analyzed during the current study are available from the corresponding author on reasonable request.

Declarations

Ethics approval and consent to participate

This study was approved by the Research Ethics Committee of the Faculty of Medicine at Alexandria University in Egypt on 16 August 2018 (reference number is 0201133). All patients included in this study gave written informed consent to participate in this research.

Consent for publication

All patients included in this research gave written informed consent to publish the data contained within this study.

Competing interests

The authors declare that they have no competing interests.

Author details

[1]Departmant of Diagnostic and Interventional Radiology, Faculty of Medicine, Alexandria University, Alexandria, Egypt. [2]Surgery Department, Faculty of Medicine, Alexandria University, Alexandria, Egypt.

Received: 29 November 2020 Accepted: 25 April 2021
Published online: 17 May 2021

References

1. Sonavane SK, Menias CO (2014) Imaging biliary strictures--a pictorial review. Curr Probl Diagn Radiol 43(1):14–34

2. Singh A, Gelrud A, Agarwal B (2015) Biliary strictures: diagnostic considerations and approach. Gastroenterol Rep 3(1):22–31
3. Bao TM, Walshe MB, Rcsi F, Roshni Patel M, Chang SD (2016) Imaging of the biliary tree: infection, inflammation and infiltration. Appl Radiol 45(4):20–24
4. Schindera ST, Miller CM, Ho LM, DeLong DM, Merkle EM (2007) Magnetic resonance (MR) cholangiography: quantitative and qualitative comparison of 3.0 tesla with 1.5 tesla. Investig Radiol 42(6):399–405
5. Costi R, Gnocchi A, Di Mario F, Sarli L (2014) Diagnosis and management of choledocholithiasis in the golden age of imaging, endoscopy and laparoscopy. World J Gastroenterol 20(37):13382–13401
6. Griffin N, Charles-Edwards G, Grant LA (2012) Magnetic resonance cholangiopancreatography: the ABC of MRCP. Insights Imaging 3(1):11–21
7. Nikolaidis P, Hammond NA, Day K, Yaghmai V, Wood CG 3rd, Mosbach DS et al (2014) Imaging features of benign and malignant ampullary and periampullary lesions. Radiographics 34(3):624–641
8. Tsai TH, Hsu JS, Lai ML, Liu GC, Shih MC, Chen CY (2016) Added value of diffusion-weighted imaging to MR cholangiopancreatography for the diagnosis of bile duct dilatations. Abdom Radiol (NY) 41(3):485–492
9. Lee NK, Kim S, Kim DU, Seo HI, Kim HS, Jo HJ et al (2015) Diffusion-weighted magnetic resonance imaging for non-neoplastic conditions in the hepatobiliary and pancreatic regions: pearls and potential pitfalls in imaging interpretation. Abdom Imaging 40(3):643–662
10. Huang WC, Sheng J, Chen SY, Lu JP (2011) Differentiation between pancreatic carcinoma and mass-forming chronic pancreatitis: usefulness of high b value diffusion-weighted imaging. J Dig Dis 12(5):401–408
11. Choi KS, Lee JM, Joo I, Han JK, Choi BI (2015) Evaluation of perihilar biliary strictures: does DWI provide additional value to conventional MRI? AJR Am J Roentgenol 205(4):789–796
12. Cetiner-Alpay Z, Kulali F, Semiz-Oysu A, Bukte Y, Ozdil K (2017) The role of magnetic resonance cholangiopancreatography and diffusion-weighted imaging for the differential diagnosis of obstructive biliary disorders. SA J Radiol 21(1):1–6
13. Yu XR, Huang WY, Zhang BY, Li HQ, Geng DY (2014) Differentiation of infiltrative cholangiocarcinoma from benign common bile duct stricture using three-dimensional dynamic contrast-enhanced MRI with MRCP. Clin Radiol 69(6):567–573
14. Kim JY, Lee JM, Han JK, Kim SH, Lee JY, Choi JY et al (2007) Contrast-enhanced MRI combined with MR cholangiopancreatography for the evaluation of patients with biliary strictures: differentiation of malignant from benign bile duct strictures. J Magn Reson Imaging 26(2):304–312
15. Sim KC, Park BJ, Han NY, Sung DJ, Kim MJ, Han YE (2020) Efficacy of ZOOMit coronal diffusion-weighted imaging and MR texture analysis for differentiating between benign and malignant distal bile duct strictures. Abdom Radiol (NY) 45(8):2418–2429
16. Zhong L, Yao QY, Li L, Xu JR (2003) Imaging diagnosis of pancreato-biliary diseases: a control study. World J Gastroenterol 9(12):2824–2827
17. Rosch T, Meining A, Fruhmorgen S, Zillinger C, Schusdziarra V, Hellerhoff K et al (2002) A prospective comparison of the diagnostic accuracy of ERCP, MRCP, CT, and EUS in biliary strictures. Gastrointest Endosc 55(7):870–876
18. Yoo RE, Lee JM, Yoon JH, Kim JH, Han JK, Choi BI (2014) Differential diagnosis of benign and malignant distal biliary strictures: value of adding diffusion-weighted imaging to conventional magnetic resonance cholangiopancreatography. J Magn Reson Imaging 39(6):1509–1517
19. Lee NK, Kim S, Kim GH, Kim DU, Seo HI, Kim TU et al (2012) Diffusion-weighted imaging of biliopancreatic disorders: correlation with conventional magnetic resonance imaging. World J Gastroenterol 18(31): 4102–4117

Publisher's Note